Predicting Seafloor Facies from Multibeam Bathymetry and Backscatter Data

Peter Dartnell and James V. Gardner

Abstract

An empirical technique has been developed that is used to predict seafloor facies from multibeam bathymetry and acoustic backscatter data collected in central Santa Monica Bay, California. A supervised classification used backscatter and sediment data to classify the area into zones of rock, gravelly-muddy sand, muddy sand, and mud. The derivative facies map was used to develop rules on a more sophisticated hierarchical decision-tree classification. The classification used four images, the acoustic-backscatter image, together with three variance images derived from the bathymetry and backscatter data. The classification predicted the distribution of seafloor facies of rock, gravelly-muddy sand, muddy sand, and mud. An accuracy assessment based on sediment samples shows the predicted seafloor facies map is 72 percent accurate.

Introduction

Mapping surficial seafloor facies (sand, silt, muddy sand, rock, and others) should be the first step in marine geological studies and is crucial when modeling sediment processes, pollution transport, deciphering tectonics, and defining benthic habitats. Traditionally, the surficial facies of the seafloor is determined by collecting a suite of bottom samples, analyzing the samples for grain size and/or determining rock type, and then mapping the results by interpolating or extrapolating the gaps between samples. However, a detailed surficial facies map is rarely achieved because generally too few samples are collected to adequately describe the variability of the surficial facies. Within the last few decades, acoustic systems have been developed that collect wide swaths of seafloor data and can map 100 percent of a study area. The most commonly used of these systems are sidescan sonars and many attempts have been made to transform the acoustic signals from these into geological and biological meaningful information (Reed and Hussong, 1989; Tamsett, 1993; Chavez and Gardner, 1994; Davis, *et al.*, 1996; Blondel and Murton, 1997; Barnhardt, *et al.*, 1998; McRea, *et al.*, 1999; Cochrane and Lafferty, 2002).

The advent of high-resolution multibeam echosounders (MBES) in the last decade has provided a new technique to efficiently map large areas of the seafloor at meter-scale horizontal, and centimeter-scale vertical resolutions (Hughes Clarke, *et al.*, 1996; Hughes Clarke, 2000a; Hughes Clarke, 2000b). The most advanced MBES systems collect a swath of georeferenced soundings that provide geodetic-quality bathymetry as well as calibrated acoustic backscatter values co-registered with each of the bathymetric soundings. High-resolution MBES systems are presently in use by most of the world's hydrographic services, commercial marine surveyors, and navies because of their accuracies, high-sounding densities, and their ability to efficiently cover 100 percent of the seafloor. MBES systems are now gaining favor with the scientific community for the same reasons. However, as with all remote sensing data, these data require adequate ground truth to derive geologically meaningful maps from them. Whereas several studies use MBES data to outline geomorphic providences on the seafloor (Goff, *et al.*, 1999; Van De Beuque, *et al.*, 1999; Gardner, *et al.*, 2001), few studies have used the MBES bathymetry and acoustic backscatter data together to classify seafloor facies on a pixel by pixel basis, thus utilizing the full resolution of the MBES data (Mitchell and Hughes Clarke, 1994; Hughes Clarke, *et al.*, 1996; Keeton and Searle, 1996), and we are unaware of any studies that have predicted seafloor facies from MBES bathymetry and acoustic backscatter data on a pixel by pixel basis, and validated the results with a quantitative accuracy assessment.

This study outlines an empirical technique that uses high-resolution multibeam bathymetry and co-registered calibrated backscatter correlated to ground truth sediment samples to predict the distribution of seafloor facies for a large area offshore Los Angeles, California. The technique uses a series of procedures that involve supervised classification and a hierarchical decision-tree classification that are now available in advanced image analysis software packages. Derivative variance images of both bathymetry and acoustic backscatter are calculated from the MBES data and then used in a hierarchical decision-tree framework to classify the MBES data into areas of rock, gravelly-muddy sand, muddy sand, and mud. A quantitative accuracy assessment on the classification results is performed using ground truth sediment samples. The predicted facies map is also ground truthed using bottom photographs and high resolution sub-bottom seismic profiles.

Study Area

The focus of the study is a marginal plateau, informally called Short Bank, located in central Santa Monica Bay, offshore Los Angeles (Figure 1). Short Bank was chosen for this study because of the large amount of seafloor data available, including high-resolution multibeam bathymetry and acoustic backscatter, sediment samples, seafloor photographs, and seismic profiles. Also, Short Bank supports a variety of benthic organisms and fish, including brittlestars, Gorgonian corals, rockfish, and sand dabs (Allen, *et al.*, 1976; Bascom, 1981) that are the focus of ongoing habitat studies. Short Bank is a relatively shallow continental shelf region (40 to 110 m deep) that projects more than 18 km out from the coastline

U.S. Geological Survey, 345 Middlefield Rd., MS-999, Menlo Park, CA 94025, (pdartnell@usgs.gov).

J.V. Gardner is presently with the Center for Coastal and Ocean Mapping, University of New Hampshire, 24 Colovos Rd., Durham, NH 03824 (jim@ccom.unh.edu).

Photogrammetric Engineering & Remote Sensing
Vol. 70, No. 9, September 2004, pp. 1081–1091.

0099-1112/04/7009–1081/$3.00/0
© 2004 American Society for Photogrammetry and Remote Sensing

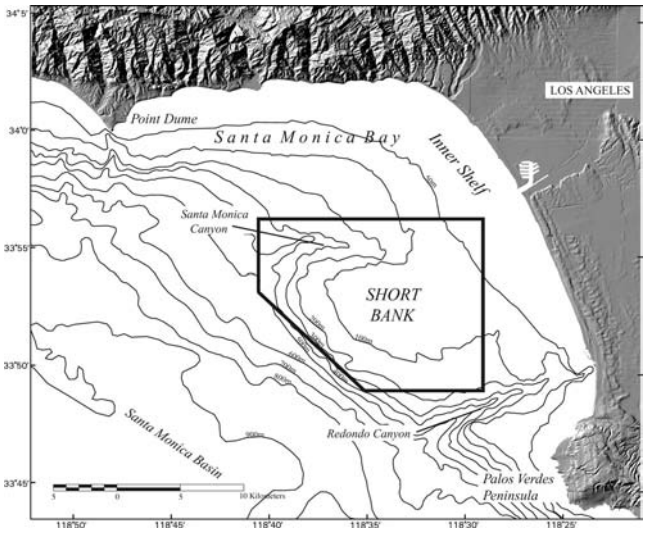

Figure 1. Study area within Santa Monica Bay, offshore Los Angeles California. The polygon indicates the extent of the study area. Isobaths are in meters.

and is bounded by two large submarine canyons: Santa Monica Canyon on the north and Redondo Canyon on the south (Gardner, *et al.*, 2003). The total study area covers 167.2 km^2 in water depths that range from 40 m on the east to 450 m on the northwest. Previous work on and around Short Bank using seismic profiles and sediment samples identified rocky outcrops with as much as 12 m of relief, as well as areas of coarse-gravelly sand, muddy sand, and sandy mud (Shepard and MacDonald, 1938; Terry and Stevenson, 1957; Junger and Wagner, 1977; Haner and Gorsline, 1978; Vedder, *et al.*, 1986; and Kolpack, 1987).

Data

Multibeam bathymetry and calibrated acoustic backscatter data (Figure 2) were collected using a Kongsberg Simrad EM1000© MBES (Gardner, *et al.*, 2003). A MBES system involves the integration of four subsystems; the multibeam transmitter/receiver electronics, a DGPS-aided inertial navigation system, a vehicle-motion sensor, and a sound-speed profiler. The 95 kHz MBES transmitter/receiver used for this study was designed for operation in water depths from 5 to 800 m. The spacing between soundings (beam footprint) is a function of receiver beam width, water depth, and angle of incidence, and varied in the study area from approximately 3.6 to 40.5 m, from 40 to 450 m water depths, respectively. The navigation subsystems provided horizontal position accuracies of better than ±1 m. A vehicle motion sensor was used to compensate for the ship's roll and pitch during transmit and receive cycles with an accuracy of ±0.02° and yaw (heading) to ±0.05°. A conductivity, temperature, and depth instrument (CTD) was used to determine the sound speed within the water column several times each day so that each acoustic path could be ray traced to the seafloor to correct for refraction in the water column. In addition, sound speed at the transducer was continuously monitored. Shipboard processing corrected backscatter levels for source level, angular response, spherical spreading, attenuation in the water column, beam pattern, and ensonified area. Bathymetry data were corrected for measured tides that referenced all depth measurements to a mean-lower, low-water datum.

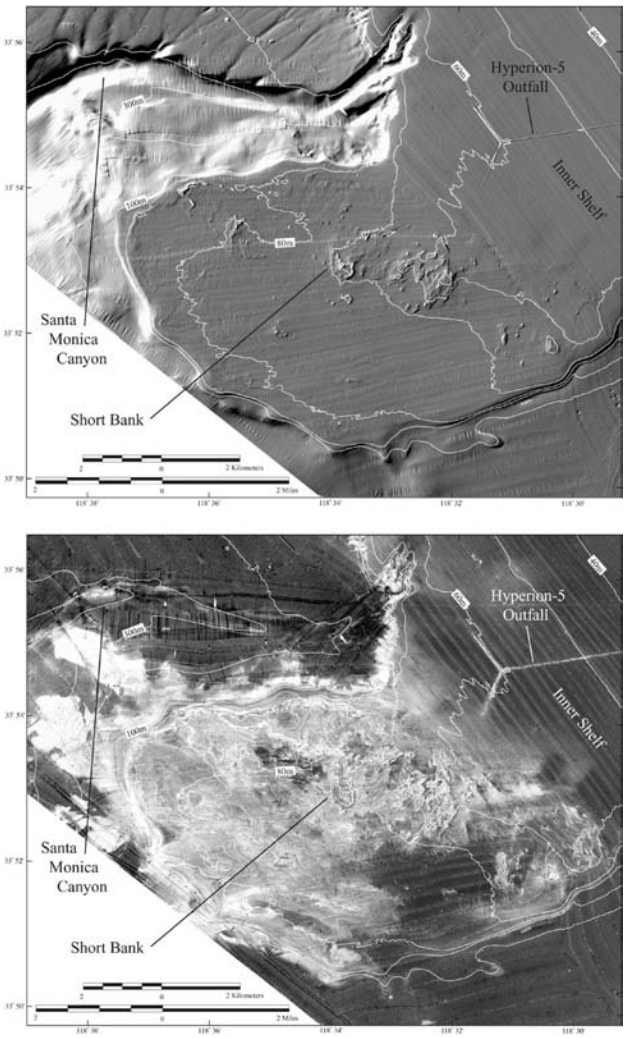

Figure 2. Multibeam shaded-relief bathymetry (top) of Short Bank and surrounding seafloor, including the inner shelf and Santa Monica Canyon (Gardner, *et al.*, 2003). Illumination azimuth, 315°, elevation 45°. Acoustic backscatter imagery (bottom) of Short Bank and surrounding seafloor including the inner shelf and Santa Monica Canyon. Light tones indicate a strong backscatter signal and darker tones indicate weaker backscatter signals. Isobaths are in meters. The linear feature in the northeast corner is the Hyperion-5 outfall pipe.

Although bathymetry can be interpreted using relatively straightforward geomorphological principles, the interpretation of acoustic backscatter is more complicated because it represents a complex interaction between the acoustic pulse and the seafloor, as well as the subsurface. Backscatter strength is dependent on the acoustic source level, the frequency used to image the seafloor (95 kHz for this study), the grazing angle, the composition of the seafloor including, grain size, water content, bulk density, seafloor roughness, and volume reverberations to within a few meters depth (Urick, 1983; Gardner, *et al.*, 1991; Augustin, *et al.*, 1996; Blondel and Murton, 1997).

Backscatter strength varies with grazing angle across track (Jackson, 1994). However, because each EM1000 backscatter value is co-registered with a sounding, the backscatter strength

is adjusted across-track by applying a Lambertian correction that uses both calculated grazing angle and measured seafloor slope. In addition to adjusting the backscatter angular response, further post-processing during the Santa Monica Bay survey removed residual acoustic ripples on the transmit to receive beam pattern product. This was done by stacking several thousand pings to average out the across-track ripple variability (Hughes Clarke, personal communication, December 2002). Once both corrections are applied, the backscatter signal better represents the across-track seafloor response to 95 kHz sound.

Finally, backscatter strength was converted from decibels (dB) to a non-dimensional 8-bit digital number (DN) using the conversion,

$$DN = 255 - (dB \times 2) \quad (1)$$

where DN ranges from 0 to 255 and dB ranges from −127 to 0. For a more in-depth discussion of multibeam systems see Hughes Clarke, *et al.*, (1996).

Individual soundings were gridded using a Butterworth distance-weighted interpolation algorithm (Diaz, 1999). The interpolation-determined cell values using a linear-weighting function that decays from a value of 1 at the grid node to nearly zero at a specified distance from the node. Therefore, individual soundings close to the cell had a higher influence on the cell's value than soundings farther away. A cell size was chosen to be no smaller than the acoustic footprint on the seafloor.

Ground truth data used in this study primarily included 60 sediment samples collected from the surface layer of box corers, but 35 mm color bottom photographs collected from a towed camera sled, and 53 km of high-resolution Huntec DTS seismic-reflection profiles were also used as ground-truth.

Classification Process

The prediction of the distribution of seafloor facies from multibeam data required a two-step empirical process that involved two classification procedures. The first step used a supervised classification of the acoustic-backscatter with grain-size data and rock locations, and the second step used those results as rules for a hierarchical decision-tree classification that included both bathymetry and acoustic backscatter. Although the hierarchical decision tree is a classification process in its own right, it is difficult to develop rules for the classification without some prior knowledge of the composition of the seafloor.

Grain-size analyses from the 60 samples were used to divide the samples into percentages of gravel, sand, and mud. Four sediment classes (facies) were identified using the Folk (1954) Classification (Table 1): gravelly muddy sand that has greater than 5 percent gravel, greater than 50 percent sand, and less than 50 percent mud; muddy sand that has less than 5 percent gravel, greater than 50 percent sand, and less than 50 percent mud; sandy mud that has less than 5 percent gravel, less than 50 percent sand, and greater than 50 percent mud; and mud that has less than 5 percent gravel, less than 10 percent sand and greater than 90 percent mud. The initial supervised classification of the acoustic backscatter data was made using the four sediment facies plus a rock facies. Rock was defined as a very high-backscatter surface with high-bathymetric relief as identified from the multibeam bathymetry data.

A *seed* pixel within the backscatter image was defined as the 8-bit-backscatter value at each of 48 sediment-sample locations (12 samples were held back for an accuracy assessment). Each seed pixel was used as the center of a *training sample* around the location of each sediment sample. A training sample is a polygon with a maximum number of pixels that have a defined range of backscatter from the seed pixel. For this study, a Euclidian distance of 400 pixels was used as the maximum number of pixels and the backscatter range was ±5 DN from the seed pixel DN. A training sample can be any shape of pixels and can vary in the total number of pixels up to a maximum of 400. For example, a training sample built from a seed pixel in a uniform region may contain 400 pixels because all the surrounding pixels are within the ±5 DN range of the seed pixel DN. However, a training sample built from a seed pixel in a highly variable area may contain only 100 pixels because only 100 pixels are within the ±5 DN backscatter range of the seed pixel DN. The maximum number of pixels and backscatter-range values were determined from trial-and-error tests to determine an internally uniform section of seafloor around each seed pixel. A backscatter range of ±5 DN about the seed pixel DN was chosen because it defines a homogeneous backscatter area around each seed pixel. Clear breaks in the data occur between low and high backscatter values. In some cases, a backscatter range of ±6 DN about the seed pixel DN crossed these breaks and created training samples with both low and high backscatter values, whereas an acoustic range of ±4 DN chose too small an area. A maximum of 400 pixels per location was used because clusters with more than 400 pixels grouped pixels located too far from the seed pixel, whereas values much less than 400 pixels picked too few pixels. A mean and standard deviation of DN was calculated for each training sample, and each training sample was assigned the seafloor facies class from the ground-truth point (i.e., muddy-sand, sandy-mud, and others). Finally, overall means and standard deviations of DN were calculated for each facies from all the training samples (Table 2).

Two methods were used to investigate the differences between the acoustic properties of the descriptive classes. The first method used mean backscatter of the descriptive-class training samples to investigate differences between the backscatter properties (Figure 3). The training samples for rock have the highest backscatter values and range from 203 to 211 DN, whereas the training samples for mud and sandy mud have the lowest backscatter values and range from 175 to 197 DN. The second method used a Student's T-test between the backscatter statistics of the different descriptive classes to determine whether each class was statistically dissimilar from one another (Table 3). This analysis showed that the mud and sandy-mud classes are not statistically different, so the mud and sandy-mud classes were grouped together into a single class called mud.

TABLE 1. DEFINITION OF SEDIMENT FACIES ON SHORT BANK

Facies	%Gravel	%Sand	%Mud
Gravelly Muddy Sand	>5	>50	<50
Muddy Sand	<5	>50	<50
Sandy Mud	<5	<50	>50
Mud	<5	<10	>90

TABLE 2. STATISTICS OF TRAINING SAMPLES. EACH TRAINING SAMPLE CONSISTS OF A MAXIMUM OF 400 BACKSCATTER PIXELS WITH ±5 DN VALUES AROUND A SEED PIXEL

	Rock	Gravelly Muddy Sand	Muddy Sand	Sandy Mud	Mud
Number of Training Samples	6	3	25	11	3
Mean DN	207.45	202.30	192.00	185.80	187.17
Standard Deviaton (DN)	2.73	2.00	8.45	5.15	8.96

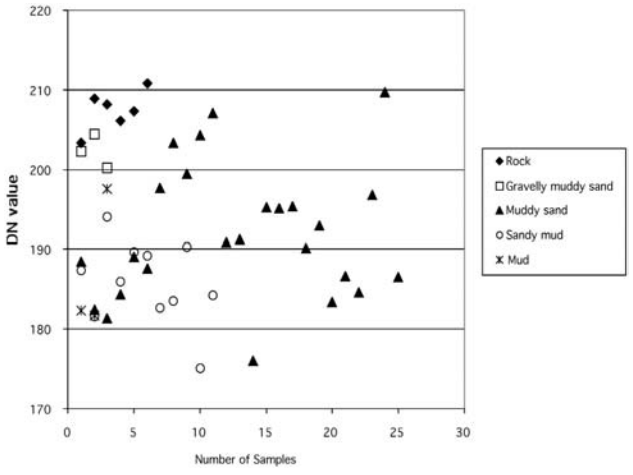

Figure 3. Scatter plot of the descriptive classes' training sample means.

TABLE 3. RESULTS OF STUDENT'S T-TESTS STUDYING THE DISSIMILARITY BETWEEN THE DESCRIPTIVE CLASSES. CLASSES ARE STATISTICALLY DISSIMILAR IF T IS GREATER THAN THE CRITICAL VALUE

Comparison	Degrees of Freedom	P	Critical Value	T
Rock vs Gravelly Muddy Sand	7	0.021	2.36	2.96
Gravelly Muddy Sand vs Muddy Sand	26	0.048	2.06	2.07
Muddy Sand vs Sandy Mud	34	0.031	2.03	2.25
Sandy Mud vs Mud	12		2.18	0.353

There are two possible explanations for the similarity between mud and sandy-mud's acoustic signals. First, the acoustic impedances (p-wave velocity $\times$ bulk density) of the finer grain-size classes may be similar. The second reason may be that there were too few mud samples to statistically distinguish between the mud and sandy-mud classes.

Once all the training samples were selected, a supervised classification was run on the entire backscatter image. The

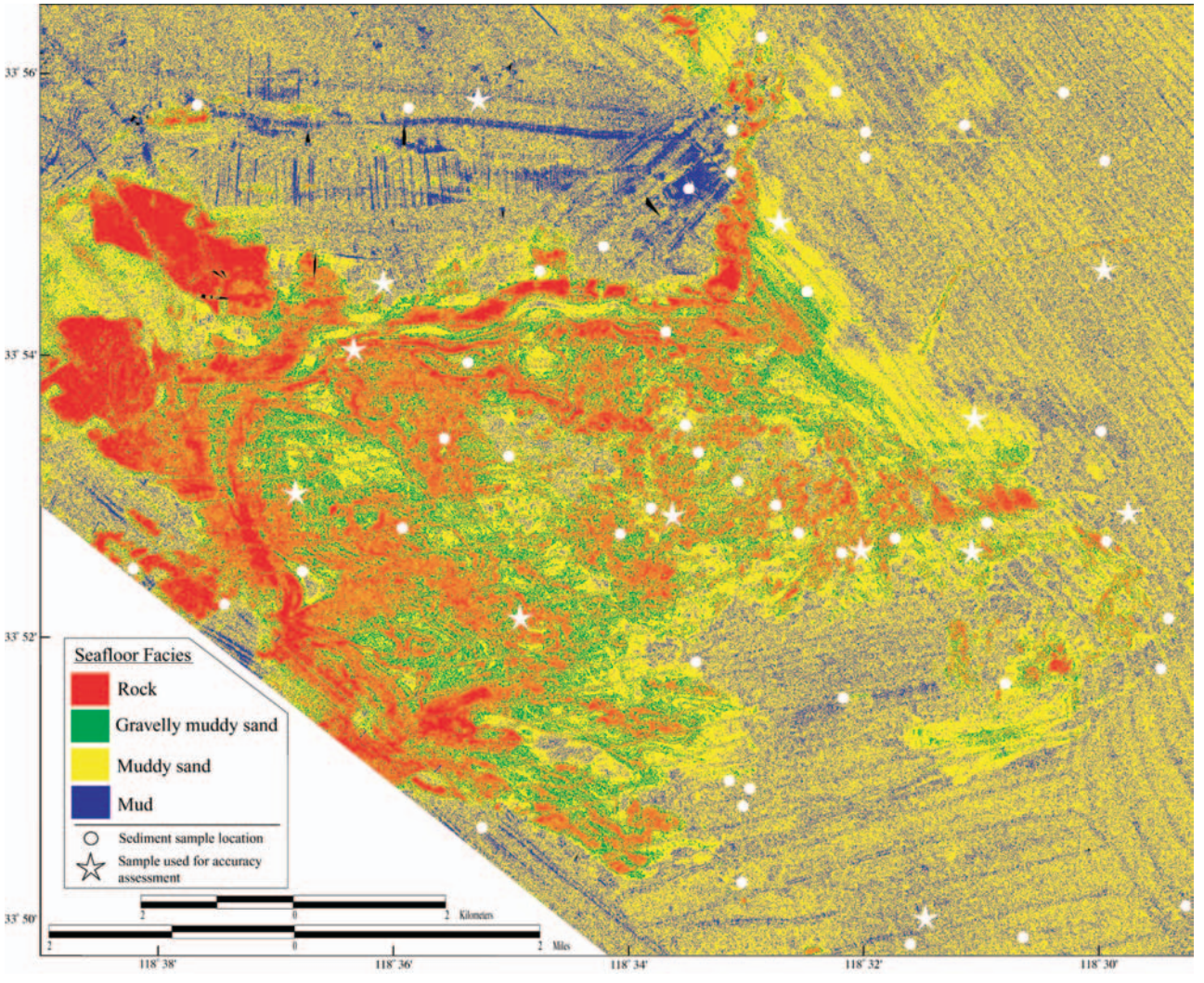

Plate 1. Predicted seafloor facies from the supervised classification.

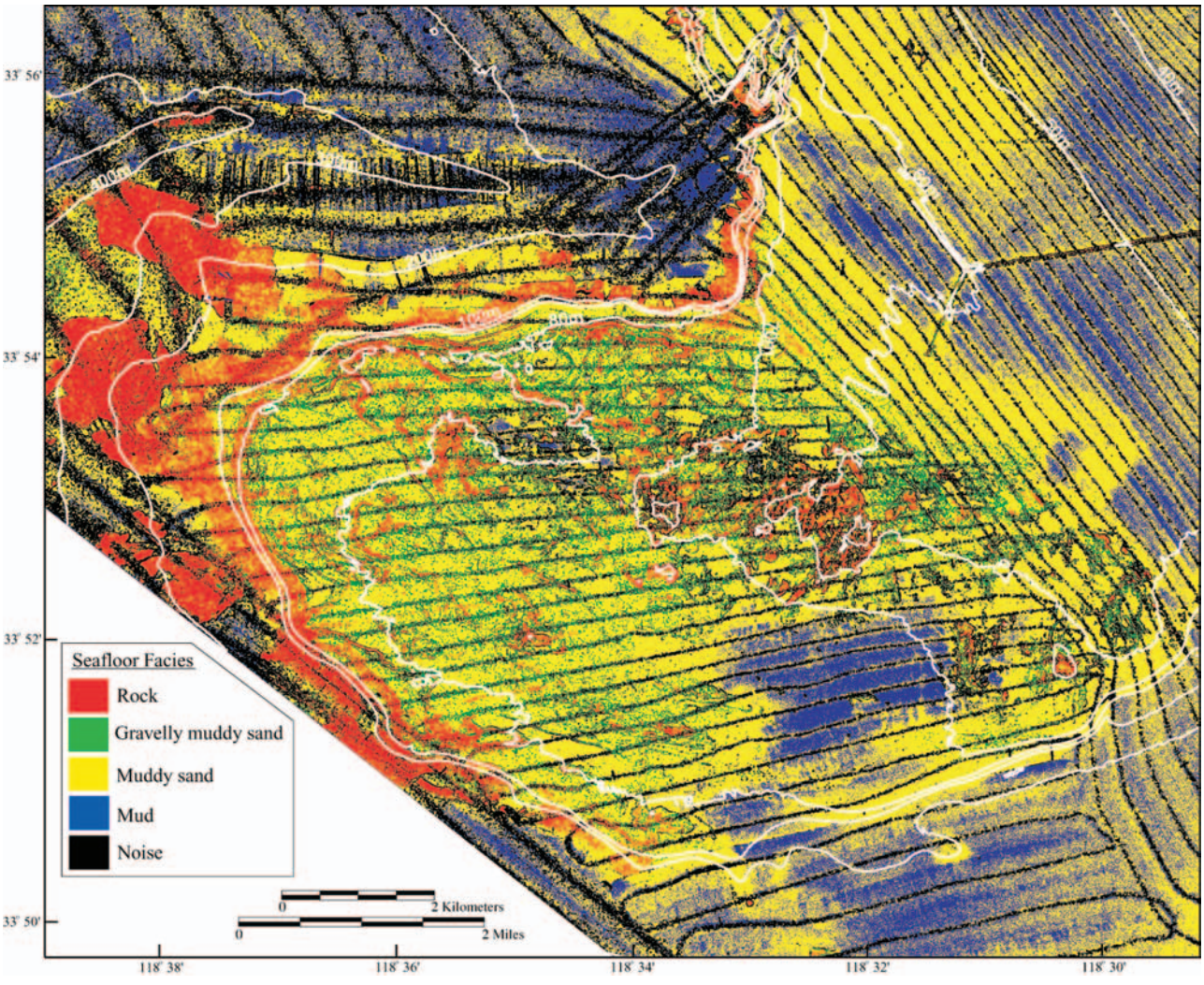

Plate 2. Predicted seafloor facies of Short Bank and surrounding region with noise class.

same constraints of a Euclidian distance of 400 pixels and a backscatter range of ±5 DN about each pixels value was used to classify each pixel in the image. This analysis assigned each pixel in the image to the training class that statistically is closest to its mean and standard deviation of backscatter. The covariance was used to correlate mean and standard deviation for each cluster to the closest training class. Each pixel in the image was assigned to one of the four seafloor classes. Finally, for visual display, each seafloor class was assigned a color to show the distribution of predicted seafloor facies (Plate 1).

A quantitative accuracy assessment was calculated on this preliminary predicted facies map to test the overall accuracy of the supervised classification. The 12 samples withheld for the assessment were picked as stratified random samples that consisted of three rock, one gravelly-muddy sand, four muddy sand, and four mud. Visual inspection determined whether the backscatter pixel at each accuracy assessment sample location was correctly classified. The accuracy assessment determined that 7 of the 12 classified map locations or 58 percent were correctly classified. One rock sample was misclassified as gravelly-muddy sand; the gravelly-muddy sand was misclassified as rock, and three mud samples were misclassified as muddy sand.

The predicted seafloor facies map generated from the supervised classification was used to test and refine the hierarchical decision-tree classification. This process used both the multibeam bathymetry and backscatter data to classify the data into the same four seafloor facies (rock, gravelly-muddy sand, muddy sand, and mud). In addition, noise was added as a fifth class. Noise is defined as the abnormally high backscatter signal recorded at the MBES nadir. At near-vertical incidence, almost all of the transmitted acoustic pulse is returned to the transducer, resulting in a saturation of the signal in the inner beams. This noise signal can be seen in Figure 2 as linear tracks of high backscatter compared to the surrounding levels.

The decision-tree classification process used four raster images, the original backscatter-intensity image, and three derivative raster images calculated from the original bathymetry and backscatter images; a 3 × 3-filtered bathymetry-variance image, an 11 × 11-filtered bathymetry-variance image, and a 3 × 3-filtered backscatter-variance image. Variance was calculated as the variability of bathymetry or backscatter within a kernel. An area with a large range of bathymetric relief, such as a rocky outcrop, would have a large bathymetry variance. A smooth area would have low bathymetry variance. Backscatter (BS) was parsed in a similar fashion; an area with high

backscatter variability, such as an outcrop (high BS) with pockets of sediment (low BS) would have a large backscatter variance, whereas a flat, uniformly-sedimented seafloor would have a low backscatter variance. The variance images were calculated by generating two intermediate images, a maximum image and a minimum image. The maximum image was calculated by running a filter (3×3 cells for 3×3 bathymetry variance and backscatter variance, and 11×11 cells for 11×11 bathymetry variance) that returned the maximum value within a kernel to the center cell. The minimum image was calculated by running a filter that returned the minimum value within a kernel to the center cell. The variance images were created from the difference between the maximum and minimum images. Two kernel sizes (3×3 and 11×11) were run over the bathymetry data to define both the small- and large-scale variance features. The 3×3 filter defined small-scale variance features such as linear ridges, whereas, the 11×11 filter defined the large-scale variance features, such as outcrops. Unsupervised classifications run on the three variance images and on the original backscatter-intensity image clustered the pixels into five groups numbering one to five: *one* representing a very low variance/intensity, *two* representing a low variance/intensity, *three* representing a medium variance/intensity, *four* representing a high variance/intensity, and *five* representing a very high variance/intensity (Figure 4).

The four unsupervised classified images were then analyzed using a hierarchical decision-tree classification that is part of the ERDAS Imagine© 8.4 software package (ERDAS©, 1999). The classification is a rules-based approach that uses a hierarchy of conditions to parse the input data into a set of classes. The decision-tree framework was developed from empirically determined textural rules, variables, and hypotheses. An hypothesis is an output-facies class, such as muddy sand, a variable is a raster image of derived values (i.e., 3×3 bathymetry variance), and a rule is a conditional statement about the variable's pixel (data) values that describes the hypothesis. Because the four unsupervised classified images are co-registered with one another, rules can be established that relate pixel values within or between images that will ultimately classify a new seafloor-facies image. Figure 5 shows an example of a simple decision tree. If a pixel within the backscatter image has a value of 4 or 5, and the same pixel in the bathymetry variance image has a value between 1 and 3, then the pixel at that location in the new facies image will be assigned a gravelly-muddy sand class. Multiple rules and hypotheses can be linked together into a hierarchy that describes the hypothesis (Figure 6).

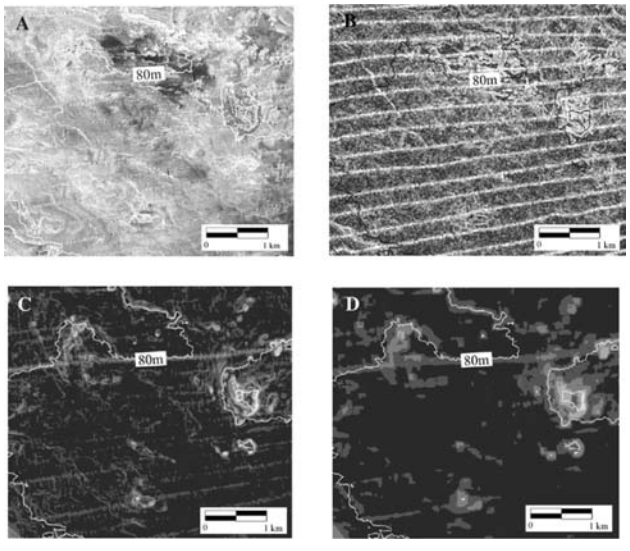

Figure 4. Four close-up views of a small area of central Short Bank. (A) backscatter intensity, (B) backscatter variance (3×3 filter) (brighter tones are areas of higher variance, whereas darker tones are areas of lower variance), (C) high-resolution bathymetric variance (3×3 filter) (brighter tones area areas of higher variance, whereas darker tones are areas of lower variance), (D) low-resolution bathymetric variance (11×11 filter).

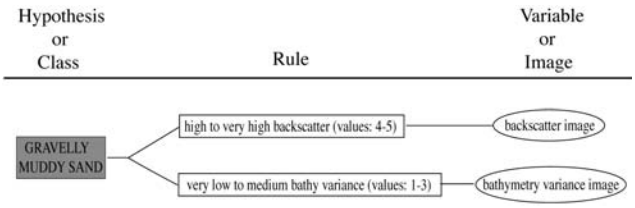

Figure 5. An example of a simple decision rule. Gravelly muddy sand is the hypothesis, high to very high backscatter and very low to medium bathymetry variance are rules, and the images are the variables.

The rules are based on the ground truth areas from the previous supervised classification. For example, it was determined that rock outcrops are exposed in the center of Short Bank at the area of very high backscatter (pixels assigned a value of 5 in the unsupervised classified backscatter image), low to very high backscatter variance (pixels assigned values between 2 and 5 in the unsupervised classified backscatter variance image), and medium to very high bathymetry variance (pixels assigned values between 3 and 5 in the unsupervised classified bathymetry variance image). It is also known that areas of the inner shelf are mainly covered in mud at the areas of low to very low backscatter (pixels assigned values of 1 or 2 in the unsupervised classified backscatter image), low to very low backscatter variance (pixels assigned values of 1 or 2 in the unsupervised classified backscatter variance image), and low to very low bathymetry variance (pixels assigned values of 1 or 2 in the unsupervised classified bathymetry variance image). Therefore, rules were developed to correctly classify these areas. The areas that were previously unknown were similarly classified based on these same rules.

The 60 ground truth sediment samples were used to test and refine the classification. After each classifying iteration, a quantitative accuracy assessment was run that compared the predicted pixel of the new classified image to the ground truth sediment type at each sample location. If required, the decision-tree rules were refined and the database reclassified until the highest accuracy assessment, 72 percent, was obtained for the ground-truth samples. The classification process resulted in a new predicted seafloor-facies thematic map composed of rock, gravelly-muddy sand, muddy sand, mud, and noise (Plate 2).

Noise was separated into its own class so it could be removed from the interpretations. The data were filtered to replace each noise pixel with the majority of non-noise pixels that surround it. For example, if a noise pixel was in a field of mud, then it was replaced with a mud classification pixel value. This process removed most of the noise and resulted in

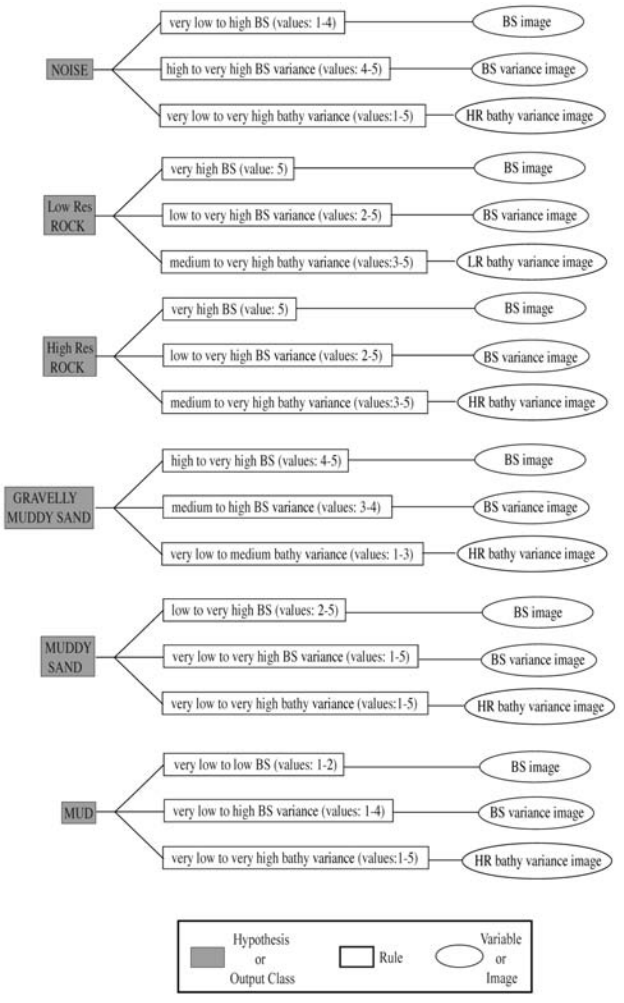

Figure 6. Complete hierarchical decision tree for predicted seafloor facies of Short Bank, Santa Monica Bay, CA. The left side boxes show the final output classes. Low Res Rock = low-resolution rock (rock defined by the 11 × 11 bathymetry variance image), High Res Rock = high-resolution rock (rock defined by the 3 × 3 bathymetry variance image). The high- and low-resolution rock classes are combined together for the final predicted seafloor faces map (Plates 2 and 3). BS = backscatter.

a predicted seafloor facies map that better represented the seafloor geology (Plate 3).

Results

The combination of hypotheses, rules, and variables in the hierarchical decision tree produced a map of predicted seafloor facies for Short Bank (Plate 3). Rock correlated with very high-backscatter, low to very high-backscatter variance, and medium to very high-bathymetry variance (Table 4). Rock has very high-backscatter because its extremely high acoustic impedance scatters all of the incident energy. Rock has a wide range of backscatter variance because many outcrops are diverse areas with exposed rock and sediment pockets that absorb some of the acoustic energy. Rock has medium to very high-bathymetry variance because exposed rock outcrops can have a wide range of relief. Gravelly-muddy sand correlated with a slightly lower backscatter than rock, medium to high-backscatter variance, and very low to medium-bathymetry variance. This sediment facies does not return as much acoustic energy as rock because some of the signal is refracted into the sediment and absorbed. Gravelly-muddy sand has medium to high-backscatter variance because the sediment is found close to the diverse outcrops, and it has very low to medium-bathymetry variance because the sediment is found on the flat plateau as well as on the transitions zones from the flat seafloor to the steep outcrops. Muddy sand correlated with the largest range of backscatter, backscatter variance, and bathymetry variance of all the facies in this area. Muddy sand has a wide range but lower backscatter than gravelly-muddy sand because its smaller grain size scatters less acoustic energy and allows more penetration, thus more volume absorption. Muddy sand is found in and around outcrops, on the steep western flanks of Short Bank, as well as on the smooth, uniform inner shelf. Mud correlated with the lowest backscatter but has a wide range of backscatter variance and bathymetry variance. Mud is similar to muddy sand, although, it has the lowest backscatter because it absorbs most of the acoustic energy because of the high water content and low density of particles in the size range of the acoustic wavelength (1.5 cm). Mud also covers a wide range of backscatter variance and bathymetry variance because it can be found trapped in pockets within the outcrops or on the smooth, uniform inner shelf.

TABLE 4. COMBINATIONS OF CLASSES USED TO DEVELOP THE PREDICTED SEAFLOOR FACIES. THE NUMBERS 1 TO 5 ARE THE RESULT OF UNSUPERVISED CLASSIFICATIONS THAT CLUSTERED THE BACKSCATTER AND VARIANCE IMAGES INTO 5 GROUPS. FIVE IS VERY HIGH BACKSCATTER OR VARIANCE, 4 IS HIGH BACKSCATTER OR VARIANCE, 3 IS MEDIUM BACKSCATTER OR VARIANCE, 2 IS LOW BACKSCATTER OR VARIANCE, AND 1 IS VERY LOW BACKSCATTER OR VARIANCE

Seafloor Facies	Relative Backscatter Intensity	Backscatter Variance	Bathymetry Variance
Rock	5	2–5	3–5
Gravelly Muddy Sand	4–5	3–4	1–3
Muddy Sand	2–5	1–5	1–5
Mud	1–2	1–4	1–5
Noise	1–4	4–5	1–5

Predicted Seafloor Facies Distribution on Short Bank

The predicted facies classification of the Short Bank area shows that Short Bank has a more complex distribution of sediment composition than does the surrounding inner shelf and deeper Santa Monica Canyon (Plate 3). Rock exposures were predicted on the seafloor throughout Short Bank and on its steeper flanks. The most prominent area of outcrops on the eastern edge of Short Bank protrudes above the surrounding seafloor by as much as 12 m (Plate 4). Predicted gravelly-muddy sand and muddy sand are found on the top flanks of the outcrops. Smaller ridges composed of individual boulders (seen in the bottom photographs) trend north to south on the western side and east to west on the northern side of Short Bank. These ridges have relatively low bathymetric relief (<2 m) compared to the larger outcrops but trend for many kilometers. Rock is also exposed in places on the steep, western flanks of Short Bank. Rock covers 18.0 km^2 or 10.8 percent of the study area.

Gravelly-muddy sand was predicted to be in small patches throughout Short Bank and only covers 13.0 km^2 or 7.8 percent of the study area. This predicted facies is generally found close to the rocky outcrops where eroded rock material has been identified (Shepard and MacDonald, 1938).

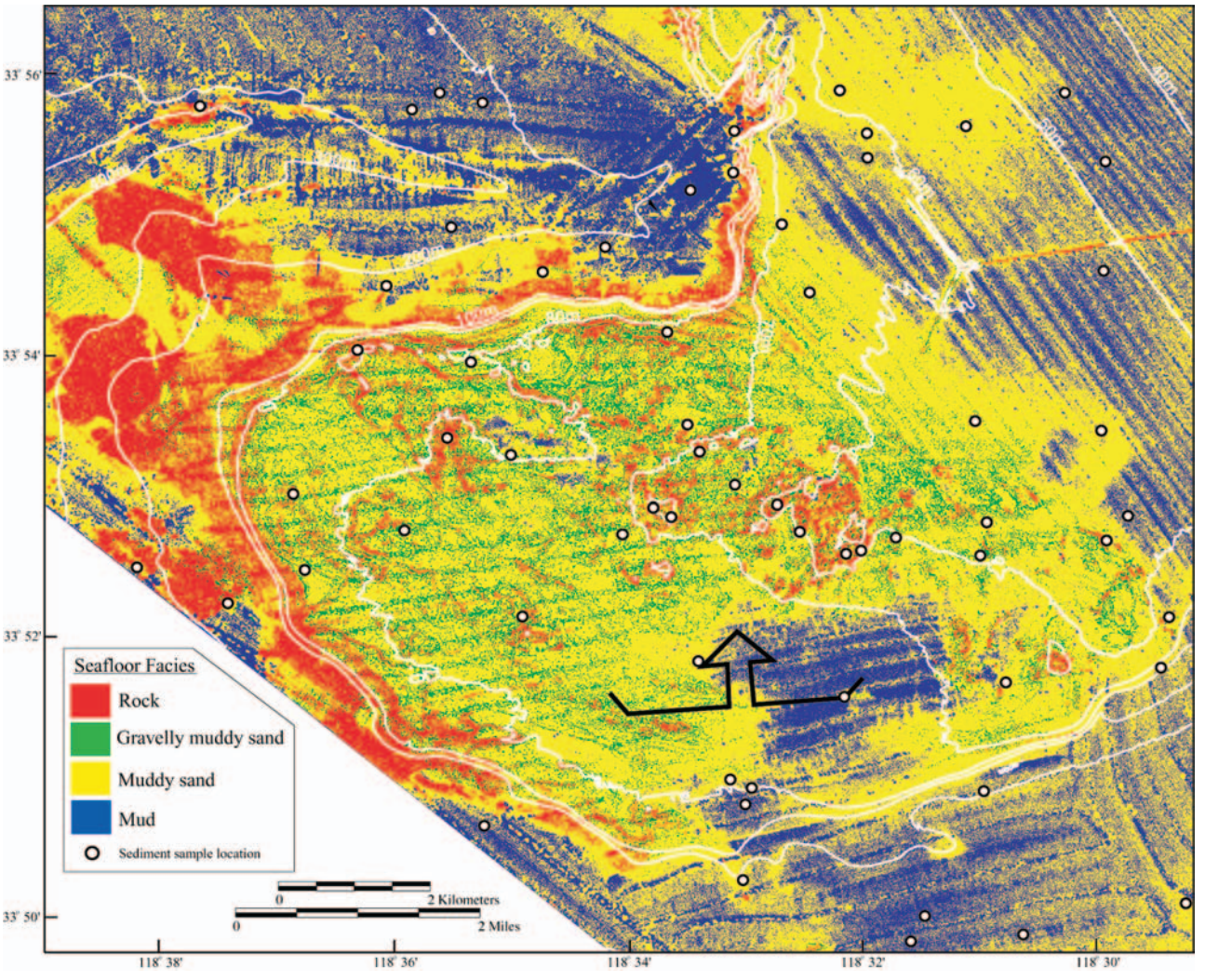

Plate 3. Predicted seafloor facies of Short Bank and surrounding region with noise class removed. The arrow shows the viewing direction of the perspective view in Plate 4.

Muddy sand is the most prevalent sediment type predicted, covering 100.7 km^2 or 60.2 percent of the area. This facies is found on the flat portion of the plateau, in pockets within the elevated rocky outcrops, on the steep flanks, and on the smooth inner shelf (Plate 3).

Predicted mud dominates the inner shelf and floor of Santa Monica Canyon. Mud was also predicted on Short Bank in small pockets within the rocky outcrops as well as in larger bathymetric lows in the center and southern portion of the plateau. Predicted mud covers 35.4 km^2 or 21.2 percent of the study area.

Accuracy Assessments

The predicted seafloor facies map was tested for validity in three ways; a quantitative accuracy assessment using sediment samples, comparisons with underwater bottom photographs, and comparisons with high-resolution, seismic-reflection profiles. The first accuracy assessment compared sediment facies of the 60 samples to the predicted seafloor facies map. Forty-three of the 60 samples (72 percent) were correctly predicted. All of the 17 misclassified samples were off by only one adjacent class (i.e., mud instead of muddy sand). In addition, there were a number of misclassifications where if the ground truth pixel location were moved over by one pixel, the classified pixel would be the correct facies.

An accuracy assessment using underwater photography shows good correlation between predicted seafloor facies and observed facies. Small rocky ridges with widths of only a few pixels on the predicted facies map are seen as areas of exposed rock (Plate 5A). The predicted facies map shows a small region of muddy sediment surrounded by coarser sand and rocks in the center of Short Bank. A bottom photograph of this area shows a field of muddy sediment with burrows and worm trails (Plate 5B). Another example is an area where the predicted facies map shows a sharp boundary between a rocky ridge and a region of muddy sand. Bottom photographs show that the ridge (Plate 5C) in this area consists of rocks from 10 to 30 cm in length with pockets of coarse sand. Photograph "D" (Plate 5D) taken approximately 3 m down track from Plate 5C over the predicted muddy sand region shows sandy sediment, but no rocks.

The third accuracy test used nine Huntec© DTS high-resolution seismic-reflection profiles to ground truth the rocky portion of the predicted facies map. Whereas the seismic data

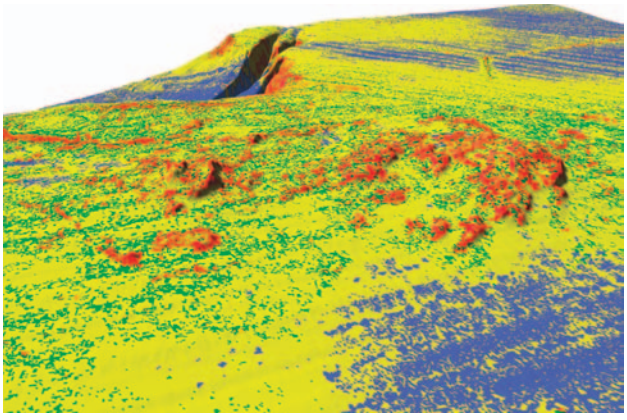

Plate 4. Perspective view of outcrops on Short Bank. Reds indicate exposed rock, green are areas of gravelly muddy sand, yellow are areas of muddy sand, and blue are areas of mud. View is looking north towards the head of Santa Monica Canyon, see Plate 3 for direction. The vertical exaggeration of the image is 10× and the distance across the bottom of the image is about 3 km.

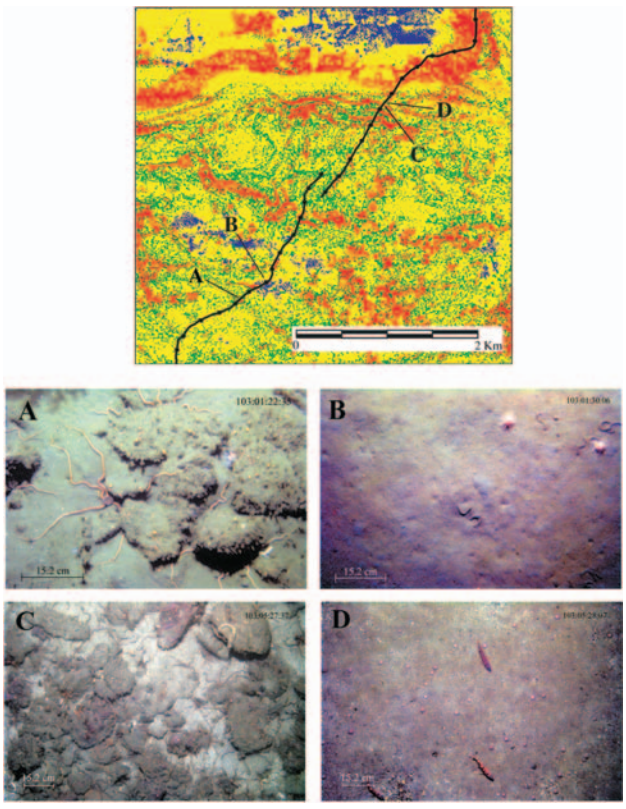

Plate 5. Comparisons between predicted seafloor facies and bottom photographs. Red in the facies map are exposed rock, green are areas of gravelly muddy sand, yellow are areas of muddy sand, and blue are areas of mud. The black line on the facies map is the camera sled path and the black dots are 5 minute markers.

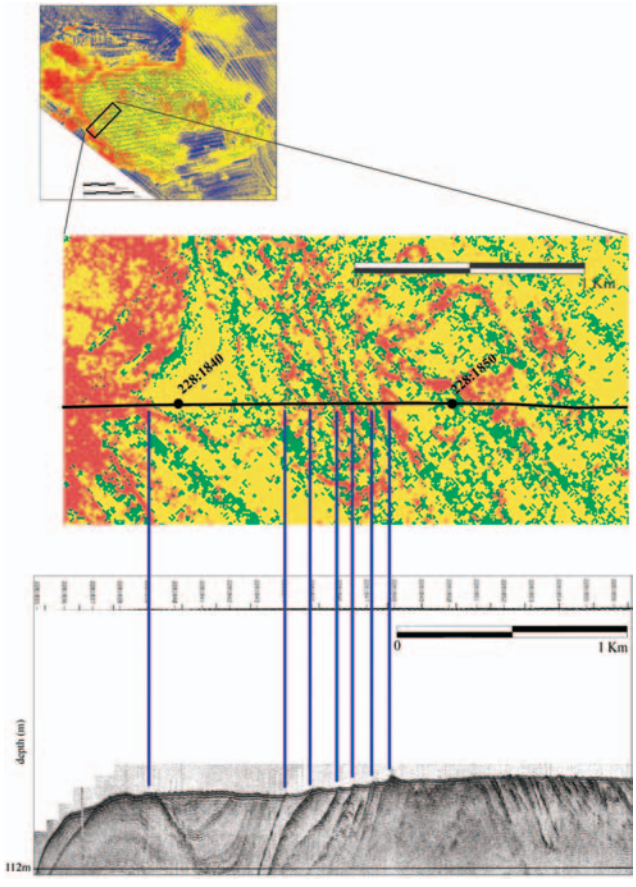

Plate 6. Comparison between predicted seafloor facies and sub-surface geology. Red in the facies map are exposed rock, green are areas of gravelly muddy sand, yellow are areas of muddy sand, and blue are areas of mud.

cannot distinguish between sediment type, they do show zones of rock outcrops and intervening sediment sections. The predicted facies map correlates with outcropping rock that stand above the sedimented regions of the plateau (Plate 6).

This technique classified the high resolution multibeam data on a pixel by pixel basis rather than interpolating between known ground truth points spaced widely apart or drawing polygons around similar ground truth points. The technique also generated more accurate results than other automated classification techniques that classify backscatter alone (50 percent accuracy for an unsupervised classification of Short Bank and 58 percent for a supervised classification).

Misclassifications

The seafloor-classification scheme predicted some misclassifications. Most of the misclassified pixels occurred near the MBES nadir that is dominated by noise. The most obvious errors are predicted rock pixels on the steep western flank of Short Bank near the MBES nadir (Plate 3). Also, the pixels at the edge of MBES nadir on top of Short Bank were misclassified as gravelly-muddy sand instead of muddy sand. The misclassification occurred because of the abnormally high backscatter from the vertical and near-vertical incidence at the MBES nadir. This high-backscatter zone rapidly decreases with across-track distance from nadir. Some of the pixels at the outer edge of the MBES nadir zone, above the noise level, have

high bathymetric variance and high backscatter similar to rock, but based on the surrounding facies, these pixels should probably be classified as muddy sand.

Conclusions

High-resolution, multibeam-echosounder data have been analyzed with remote sensing analytical techniques to generate a predicted facies map that is the most complete and accurate map of the surficial geology of the seafloor of Short Bank. A hierarchical decision tree using bathymetry and backscatter data has predicted the distribution of rock, gravelly-muddy sand, muddy sand, and mud in this region. The predicted facies were ground truthed with sediment samples, underwater photography, and seismic-reflection profiles. Ground truth with sediment samples shows that the predicted facies map is 72 percent accurate, better than other automated classification methods and good correlations are demonstrated between underwater photography and seismic-reflection profiles.

The classification technique preserves accurate geo referencing and allows the mapping of four seafloor facies. Large rock outcrops with pockets of gravelly-muddy sand, and muddy sand cover portions of the plateau. Smaller linear ridges composed of rock boulders and muddy sand extend for kilometers. Muddy sand covers the majority of the plateau and its steep flanks. Mud covers the inner shelf, small bathymetric lows on Short Bank, and the deeper Santa Monica Canyon region.

This seafloor-classification technique provides a method to transform high resolution multibeam bathymetry and calibrated acoustic backscatter data into meaningful geological information. Although this classification technique can be used on other areas of the seafloor, the exact values within the hierarchical decision tree cannot be transferred to a different area. Ground truth samples and other geological information need to be gathered for each new study area to build the area's knowledge database. The predicted-seafloor-facies map from this study can be used not only to study the spatial distribution of geologic material, but also to model sediment processes, pollution transport, and for defining benthic habitats within central Santa Monica Bay.

Acknowledgments

Thanks to Pat Chavez, Jr. and Randy Cutter for thoughtful reviews of earlier versions of this manuscript and three unidentified reviewers whose suggestions significantly improved the manuscript. Thanks to the Santa Monica Restoration Project who partially supported the work and thanks to John Hughes Clarke and Larry Mayer for discussions during the course of this study.

References

Allen, J.M., H. Pecorelli, and J. Word, 1976. Marine organisms around outfall pipes in Santa Monica Bay, *Journal WPCF*, 48:1881–1893.

Augustin, J.M., R. Le Suave, X. Lurton, M. Voisset, S. Dugelay, and C. Satra, 1996. Contribution of the multibeam acoustic imagery to the exploration of the sea-bottom, *Marine Geophysical Researches*, 18:459–486.

Barnhardt, W.A., J.T. Kelly, S.M. Dickson, and D.F. Belknap, 1998. Mapping the Gulf of Maine with side-scan sonar: A new bottom-type classification for comples seafloors, *Journal of Coastal Research*, 14:646–659.

Bascom, W., 1981. The effects of sludge disposal in Santa Monica Bay, *Impact of Marine Pollution on Society* (V.K. Tippie and D.R. Kester, editors), J.F. Bergin, South Hadley, Massachusetts, pp. 217–244.

Blondel, P., and B.J. Murton, 1997. *Handbook of seafloor sonar mapping*, John Wiley and Sons, New York, 314 p.

Chavez, P.S. Jr., and J.V. Gardner, 1994. Extraction of spatial information from remotely sensed image data—an example: GLORIA sidescan sonar images, *Canadian Journal of Remote Sensing*, 20:433–453.

Cochrane, G.R., and K.D. Lafferty, 2002. Use of acoustic classification of sidescan sonar data for mapping benthic habitat in the Northern Channel Islands, California, *Continental Shelf Research*, 22:683–690.

Davis K.S., N.C. Slowey, I.H. Stender, H. Fiedler, W.R. Bryant, and G. Fechner, 1996. Acoustic backscatter and sediment textural properties of inner shelf sands, northeastern Gulf of Mexico, *Geo-Marine Letters*, 16:273–278.

Diaz, J.V.M., 1999. *Analysis of multibeam sonar data for the characterization of seafloor habitats*, Masters Thesis, University of New Brunswick, 138 p.

ERDAS© Field Guide, 1999. ERDAS© Inc., Atlanta, Georgia, 672 p.

Folk, R.L., 1954. The distinction between grain size and mineral composition in sedimentary rock nomenclature, *Journal of Geology*, 62:344–359.

Gardner, J.V., M.E. Field, H. Lee, and B.E. Edwards, 1991. Ground-truthing 6.5-kHz side scan sonographs: What are We really imaging, *Journal of Geophysical Research*, 96:5955–5974.

Gardner, J.V., P. Dartnell, K.J. Sulak, B. Calder, and L. Hellequin, 2001. Physiography and Late Quaternary-Holocene processes of northeastern Gulf of Mexico outer continental shelf off Mississippi and Alabama, *Gulf of Mexico Science*, 19:132–157.

Gardner, J.V., P. Dartnell, L.A. Mayer, and J.E. Hughes Clarke, 2003. Geomorphology, acoustic backscatter, and processes in Santa Monica Bay from multibeam mapping, *Marine Environmental Research*, 56:15–46.

Goff, J.A., D.L. Orange, L.A. Mayer, and J.E. Hughes Clarke, 1999. Detailed investigation of continental shelf morphology using a high-resolution swath sonar survey: The Eel margin, northern California, *Marine Geology*, 154:255–269.

Haner, B.E., and D.S. Gorsline, 1978. Processes and morphology of continental slope between Santa Monica and Dume Submarine Canyons, Southern California, *Marine Geology*, 28:7787.

Hughes Clarke, J.E., L.A. Mayer, and D.E. Wells, 1996. Shallow-water imaging multibeam sonars: A new tool for investigating seafloor processes in the coastal zone and on the continental shelf, *Marine Geophysical Researches*, 18:607–629.

Hughes Clarke, J.E., 2000a. Acoustic Seabed Surveying—Meeting the new demands for Accuracy, Coverage, and Spatial Resolution, *Geomatica*, 54:473–513.

Hughes Clarke, J.E., 2000b. *Present-day methods of depth measurements, Continental shelf limits: The scientific and legal interface* (Peter J. Cook and Chris M. Carleton, editors), Oxford University Press. pp. 139–159.

Jackson, D.R., 1994. APL-UW high-frequency ocean environmental acoustic models handbook. Technical Report. APL-UW TR9407, 195 p.

Junger, A., and H.C. Wagner, 1977. *Geology of the Santa Monica and San Pedro Basins, California Continental Borderland*. U.S. Geological Survey Miscellaneous Field Studies, Map, MF-820, 5 sheets, 1 pamphlet, scale 1:250000.

Keeton, J.A., and R.C. Searle, 1996. Analysis of Simrad EM12 multibeam bathymetry and acoustic backscatter data for seafloor mapping, exemplified at the mid-Atlantic Ridge at 45°N, *Marine Geophysical Researches*, 18:663–688.

Kolpack, R.L., 1987. Sedimentology of shelf and slope in Santa Monica Bay, California, *American Association of Petroleum Geology*, 71: 578.

McRea Jr., J.E., H.G. Greene, V.M. O'Connell, and W.W. Wakefield, 1999. Mapping marine habitats with high-resolution sidescan sonar, *Oceanologica Acta*, 22:679–686.

Mitchell, N.C., and J.E. Hughes Clarke, 1994. Classification of seafloor geology using multibeam sonar data from the Scotian Shelf, *Marine Geology*, 121:143–160.

Reed, T.B., and D. Hussong, 1989. Digital image processing techniques for enhancement and classification of SeaMARC II side scan imagery, *Journal of Geophysical Research*, 94:7469–7490.

Shepard, F.P., and G.A. MacDonald, 1938. Sediments of Santa Monica Bay, California, *Bulletin of the American Association of Petroleum Geologists*, 22:201–216.

Tamsett, D., 1993. Sea-bed characterization and classification from the power spectra of side-scan sonar data, *Marine Geophysical Researches*, 15:43–64.

Terry, R.D., and R.E. Stevenson, 1957. Microrelief of the Santa Monica Shelf, California, *Bulletin of the Geological Society of America*, 68:125–128.

Urick, R.J., 1983. *Principles of underwater sound*, 3rd edition, McGraw-Hill Book Company, New York, 423 p.

Van De Beuque, S., J. Auzende, Y. LaFoy, and R. Grandperrin, 1999. Benefits of swath mapping for the identification of marine habitats in the New Caledonia Economic Zone, *Oceanologica Acta*, 22:641–650.

Vedder, J.G., H.G. Green, S.H. Clarke, and M.P. Kennedy, 1986. *Geologic Map of the Mid-Southern California Continental Margin*, California Continental Margin Geologic Map Series, Map 2A, Division of Mines and Geology, Scale 1:250000.

(Received 26 June 2002; revised and accepted 15 August 2003)